

# 1 Using Formvar to Capture Ice Crystals and Retrieve Roughness

## 2 Parameters

3 Omer Celebi<sup>1</sup>, Andrew R.D. Smedley<sup>1</sup>, Paul Connolly<sup>1</sup> Ann R. Webb<sup>1</sup>

4 <sup>1</sup>Department of Earth and Environmental Sciences, University of Manchester, Manchester, M13 9PL, UK

5 *Correspondence to:* Omer Celebi (omer.celebi@postgrad.manchester.ac.uk)

6 **Abstract.** Ice crystal roughness is a poorly observed and understood parameter, yet it significantly influences crystal's  
7 scattering properties and consequently impacts radiative transfer in the atmosphere, contributing to uncertainties in weather  
8 and climate forecasting. **In this study, we introduce a novel approach as a proof-of-concept to obtain high-resolution roughness**  
9 **measurements, building on the traditional formvar method for capturing ice crystals and validated through comparison of the**  
10 **roughness parameters of salt crystals and salt crystal replicas.** Ice crystals were grown in the Manchester Ice Cloud Chamber,  
11 collected, and subsequently imaged using various techniques, including a scanning optical profilometer, which enabled the  
12 identification of roughness features as small as 0.8  $\mu\text{m}$ . This approach provides critical insights into roughness characteristics  
13 that are significant for improving radiative transfer models and forecasts.

## 14 1 Introduction

15 The mean equilibrium surface temperature of Earth is significantly affected by clouds that are responsible for both trapping  
16 terrestrial radiation as well as reflecting solar radiation back to space. The balance between these processes determines the  
17 change in surface temperature due to changes in the cloud/ presence of the cloud (Hong Y, 2015). As indicated in the IPCC  
18 report (2013), the sensitivity in the prediction models for climate changes can reach up to 1.5°C–2.0°C. The reason for this  
19 range of estimates in the prediction of surface temperature was noted in the report as primarily being due to our limited  
20 knowledge of cloud feedback (IPCC, 2013). This lack of understanding of the physical properties of clouds is particularly  
21 acute for ice clouds since they are complex over a range of spatial scales and cover large portions of the globe, thus causing  
22 significant errors in predictions of climate change. These uncertainties have been substantially mitigated through rigorous,  
23 collaborative efforts by the research community, dedicated to advancing the understanding and precise quantification of cloud  
24 feedback mechanisms across a range of cloud regimes (IPCC, 2023). As the scientific community has worked to address these  
25 uncertainties, our focus here is on issues that can be further mitigated through a deeper understanding of the microscopic  
26 properties of ice crystals. This comprises backscattering properties of ice crystals based on their microphysical properties,  
27 including shape, orientation, complexity, and roughness.

28

29 Cloud models can give accurate results if the inputs represent the actual conditions. Therefore, there have been many efforts  
30 over the last 80 years (Bailey, et al., 2009) to understand ice crystal habit formation as a function of environmental conditions,  
31 enabling the input to cloud models to be as accurate as possible. In one of the earliest systematic investigations, Magono and  
32 Chung (1966) developed a comprehensive classification of natural snow crystal types, creating a foundational framework that  
33 has since guided research in snowflake morphology. More recently, in 2005, an experiment was conducted by Libbrecht to  
34 explain the mechanism that creates a general hexagonal prism shape for ice crystal growth when their sizes are between 10-  
35 100  $\mu\text{m}$  (Libbrecht, 2005). Also, in the same year, Connolly et al. (2005) studied the correlation between the electric field and  
36 aggregation of ice crystals and also made observations of chains of ice crystals during fieldwork into deep convective outflows.  
37 The results of the study also compared in many aspects with the work done by Saunders and Wahab (1975) since their field  
38 data were similar.

39

40 As the habit of the ice crystal varies under different conditions, its contribution to scattering behaviour and overall cloud  
41 reflection capacity varies. For example, in 2015(a), Smith et al. investigated scattering by hollow columnar crystals. These  
42 types of column crystals have hollows in their end faces that alter the scattering behaviour. It was found that the phase functions  
43 are not affected too much, but there is a difference in asymmetry parameters as a result of different reflections occurring around  
44 the hollows (Smith, et al., 2015a).

45

46 Throughout these investigations, the methods used to analyse and observe the ice crystals also developed over time as  
47 technology developed. Initially, ice crystals were able to be captured for analysis with a solution often referred to as 'formvar'.  
48 Formvar is a solution of polyvinyl formal resin (formvar) dissolved in ethylene dichloride (Schaefer, 1941). The solution is  
49 used to coat a surface and then the solvent evaporates leaving behind a plastic coating, or in the case of an ice crystal that  
50 melts, a plastic replica. Formvar, often combined with electron microscopy or other imaging techniques, has found widespread  
51 application e.g. Kahler et al. (1951) used formvar to coat copper screens for visualizing copper-cystine fibers under electron  
52 microscopy. In atmospheric science, following on from Schaeffer (1941), Rucklidge (1965) conducted an experiment that  
53 involved the use of the formvar solution to create replicas and examine size and shape properties under an electron microscope.  
54 The work of Griggs and Jayaratne (1986) led to improvements in the capture quality, as well as precautions during the  
55 application of the procedure. Since then, the method has frequently been used to create and then image replicas, sometimes  
56 using high-resolution optical microscopy, as in Smith et al (2015b) who used this technique to classify and explain the habit  
57 of crystals grown in different conditions. Finnegan and Pitter (1988) investigated the replica process to explain aggregation  
58 and secondary ice formation. In the study of Miloshevich et al. (1996), formvar was used to collect cloud particles as a part of  
59 the process for a balloon-borne cloud particle replicator to measure the vertical profile of particles. Another replicator was  
60 designed and used by Warburton et al. (1983) for the study of transmission of snowfall. This replicator also included a formvar  
61 to capture crystals by creating a thin film and allowing crystals to impact it to produce detailed imprints on the film. More

62 recently, the use of formvar for crystal habit classification has been largely superseded by optical imaging probes that offer  
63 automatic sizing and shape determination but at a lower resolution than that available from standard optical imaging of formvar  
64 replicas. These probes provide fast and in-situ imaging, but the resolution of the images is not adequate to analyse the surface  
65 details or roughness.

66 Developments of the original optical imaging probes such as the cloud particle imager (CPI) have allowed roughness to be  
67 inferred from the light scattering patterns off cloud particles using instruments such as the small ice detector (SID-3; Ulanowski  
68 et al. 2014). This technique measures the combined effect of small-scale surface roughness and the crystal complexity as the  
69 overall practical impact of ‘roughness’ on scattering but does not directly measure the small-scale roughness features. This  
70 method, and variations on SID-3, have been used airborne to measure within cirrus (Ulanowski et al. 2014; Järvinen et al.  
71 2018), and in the laboratory to determine the impact of growth conditions on crystal roughness (Voigtländer et al. 2018).  
72 Meanwhile Magee et al. (2014) grew ice crystals in the low-pressure chamber of an Environmental Scanning Electron  
73 Microscope (ESEM) and observed a wide range of surface features on scales from 100 nm to more than 10  $\mu\text{m}$  on both these  
74 and externally grown crystals transferred to the chamber. Meanwhile Collier et al. (2016) used a sand particle scanned with an  
75 Atomic Force Microscope (AFM) as a proxy for ice particle roughness parameters. The roughness values obtained from the  
76 sand grains were found to be similar to those retrieved by SID-3 for ice crystals, making sand a suitable medium for capturing  
77 roughness then applied to scattering models.

78  
79 Up to this point, a direct measurement of the surface roughness of ice crystals has been elusive, yet the traditional formvar  
80 technique has the potential to enable such measurements. There is a pioneering study that investigates the formvar replica  
81 process and its ability to capture roughness details (Agar, et al., 1956). This study used formvar solution to coat metal alloys,  
82 and an interferometer microscope was used to conduct further roughness measurements. Ideally, a uniform thickness of  
83 formvar should be present across the surface. On average, the thickness of the formvar solution achieved was around 700 Å.  
84 After the coating process, scans of the reverse of the replica and the original material were compared, and the difference  
85 between them was found to be negligible.

86  
87 To move beyond having to use proxies of roughness, in this study, we demonstrate a technique to obtain a direct measurement  
88 of the roughness of ice crystals by coupling the relatively old method of capturing ice crystals in formvar with newer  
89 instrumentation in the form of an optical profilometer. Nevertheless, using such an old technique requires some modifications  
90 to improve the quality of capture and allow for detailed imaging that then enables a direct measurement of the roughness and  
91 provides a useful complementary technique to the current suite of cloud imaging probes. Unlike the method described in Smith  
92 et al. (2015a), we introduced modifications such as increasing the amount of formvar solution used, which helped sustain a  
93 more consistent coating. Additionally, the process was carried out under a vacuum to make sure that the replicas were able to  
94 be created whose details will be explained in the methodology section.

## 95 2 Methodology

96 The formvar replica technique has traditionally been an efficient way of capturing ice crystals and preserving their surface  
97 structure, which is particularly important for ice crystals which would otherwise melt once collected and brought to laboratory  
98 temperature. While it has successfully been used for determining crystal habits and features such as hollowness, identifying  
99 roughness of a crystal requires evidence that the formvar can accurately reproduce the necessary high-resolution detail. We  
100 present the final methodology developed to determine the scale of roughness of ice crystals. The results section will also  
101 illustrate some of the intervening stages in developing the technique, for example the imaging of salt crystals as proof of  
102 concept that the formvar replicas could maintain structure of the magnitude expected of ice crystal roughness.

103  
104 **The initial step of the traditional method is the placement of a solution of 0.6 wt% polyvinyl formal resin in chloroform**  
105 **(CHCl<sub>3</sub>) by using a brush onto a glass slide that is then used to capture the ice crystals.** Once the formvar solution has  
106 subsequently dried out, a replica of the ice crystal is left in the solid formvar which can be investigated under microscopy to  
107 retrieve features of the crystal.

108  
109 The brush leaves a thin layer of solution after it is applied to the slide. This has the advantage of drying rapidly but the crystals  
110 cannot be covered fully. This results in imprints of crystals which are suitable for habit identification but not ideal for  
111 roughness detection. A more effective approach involves capturing the entire crystal by suspending and encasing it in formvar,  
112 thereby ensuring that all surface cavities remain filled during the solidification of the solution and the sublimation or ablation  
113 of the crystal. As most of the crystals generated in the Manchester Ice Cloud Chamber (MICC) fall under 1 mm in size, that  
114 depth of solution was targeted for the experiment, but brings its own challenges.

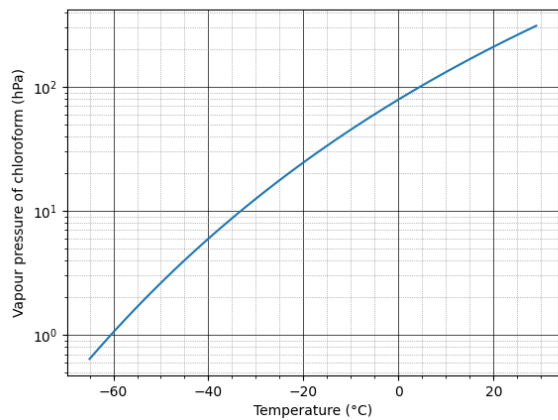
115  
116 In order to achieve the increased thickness of formvar solution required, aluminium foil was used to create a wall around the  
117 glass slide, creating a pool of the solution to a desired level of thickness. It is critical to have enough depth for ice crystals to  
118 submerge fully but the evaporation of the chloroform solvent from a thicker layer of formvar, at the low temperatures required  
119 for crystal formation, proved too slow at standard atmospheric pressure. Early trials found that the chloroform could not  
120 completely evaporate before the crystals deformed or ablated.

121  
122 The study of Kawamura et al (1987) shows the evaporation rate per unit area is calculated following Eq. (1):

$$123 E = k * M * P(T_s) / RT \quad (1)$$

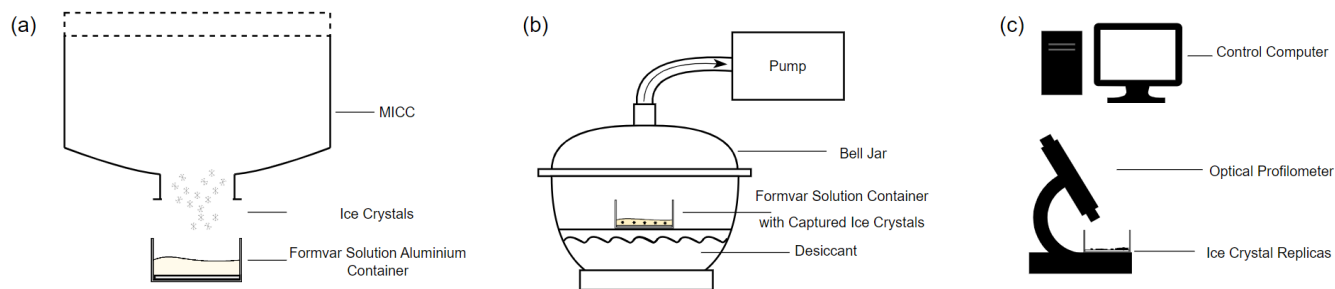
124 Where  $k$  is the mass transfer coefficient,  $M$  is the molecular weight,  $P(T_s)$  is the vapour pressure at  $T_s$  which is the temperature  
125 of solution surface, while  $R$  and  $T$  are the gas constant and absolute temperature of air respectively. The evaporation rate is  
126 directly proportional to vapour pressure, thus at a given temperature increasing the vapour pressure increases the evaporation

127 rate. As seen in Figure 1 at a temperature of  $-20^{\circ}\text{C}$ , the vapour pressure of chloroform is decreased by a factor of at least 5.5  
128 when compared to room temperature.  
129



130  
131 **Figure 1.** Vapour pressure of chloroform (hPa) vs temperature ( $^{\circ}\text{C}$ ) adapted from Cheric (1995).

132  
133 This suggests a solution to the problem caused by slow evaporation of chloroform: that by reducing the external pressure on  
134 the slide the evaporation rate would be increased. Accordingly, the formvar slide, with its captured ice crystals was sealed  
135 inside a bell jar and air slowly pumped from within. The target pressure was 140–200 hPa achieved at a flowrate (set to 10  
136  $\text{m}^3\text{min}^{-1}$ ) that would not disturb the sample contained within the bell jar.  
137



138  
139  
140 **Figure 2.** Schematic (not to scale) showing steps described in methodology: **(a)** sample collection, **(b)** evaporation process, and **(c)** optical  
141 profilometer scanning.

142 At this flowrate, it took a few minutes to reach the desired pressure level, and once it was reached, the evaporation visually  
143 inspected: as the evaporation occurs, the colour of the solution goes from transparent to silky white. The sample was left to  
144 evaporate for 10 minutes to ensure the process was complete.

145

146 Samples were initially examined using an optical profilometer, specifically the Keyence X200K 3D Laser Microscope with a  
147 lateral resolution less than 10 nm and vertical resolution less than 5nm, to ensure that the crystal replicas remained intact  
148 without undergoing any additional deformations. This preliminary inspection enabled the identification of areas of interest for  
149 more detailed analysis. Once selected, these areas were thoroughly surface scanned using the same instrument, and the resulting  
150 scan data was stored for further evaluation. The primary advantage of utilizing the optical profilometer over earlier imaging  
151 techniques lies in its dual functionality. It offers a rapid initial optical assessment, followed by a highly detailed 3D surface  
152 scan that captures intricate topographical features with precision. The optical profilometer, such as a laser scanning confocal  
153 microscope, utilizes non-contact techniques to measure surface profiles, roughness, and thickness across different materials.  
154 It employs both laser and white light sources to simultaneously capture laser intensity, colour, and height data, allowing for  
155 the generation of fully focused colour images and detailed 3D height profiles. In contrast to traditional methods like scanning  
156 electron microscopy, which may distort samples due to electron beam interaction, the profilometer maintains sample integrity  
157 while delivering high-resolution data. This capability makes it well-suited for both quick assessments and comprehensive  
158 surface analysis, providing excellent versatility and accuracy, compared to other methods used in the early stages of technique  
159 development. After the scanning data was retrieved, it was examined and analysed using a software package called Gwyddion.  
160 This program allows users to import surface scanning data and to focus on extracting detailed data from a specified area of the  
161 scanned surface, in this case the crystal replicas and not the surrounding formvar, though background areas of formvar were  
162 scanned to provide a baseline roughness value. It enables parameters like mean roughness to be calculated following Eq. (2):

$$163 R_a = \frac{1}{L} \int_0^L |Z(x)| dx \quad (2)$$

164

165 Where L is evaluation length and Z(x) is height profile (Gadelmawla, et al., 2002) and root mean square (RMS) roughness is  
166 calculated following Eq. (3):

$$167 R_q = \sqrt{\frac{1}{L} \int_0^L Z(x)^2 dx} \quad (3)$$

### 168 3. Results and Discussion

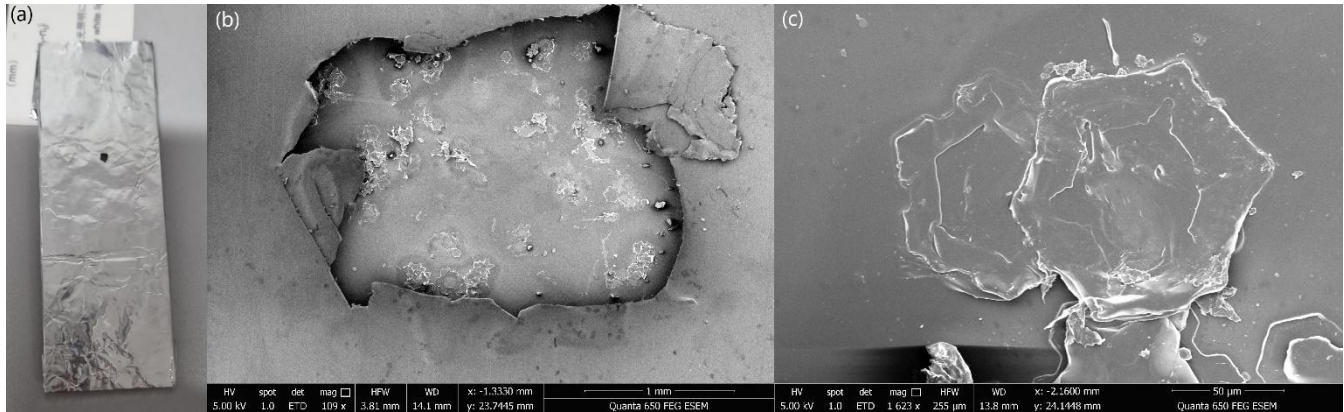
169 The methodology outlined in the previous section was developed to demonstrate that it is possible to extract roughness  
170 information directly from ice crystals formed within clouds. It was inspired by the observation that traditional optical  
171 microscope images are not sufficiently detailed to provide information on roughness as the required high image resolution  
172 cannot be achieved. During the initial examination of the optical microscope sample images retrieved using the brush  
173 technique, there were features observed that could be artefacts of the formvar process itself, rather than features of the original  
174 crystals. Clarifying whether these are artefacts or belong to the crystals themselves, however, requires high-resolution images.

175

176 Initially, scanning electron microscopy (SEM) was employed to capture the high-resolution images necessary for the analysis  
177 by scanning the surface of the material with a focused beam of electrons. SEM was chosen for its ability to achieve resolutions  
178 of up to approximately 100 nm, which theoretically provides sufficient detail to meet the 100nm roughness measurement goal.  
179 While SEM was not used directly for surface roughness measurement purposes in this study, it played a critical role in the  
180 preliminary phase by allowing for detailed characterization and identification of artefacts introduced during the preliminary  
181 formvar replication. The ability to distinguish artefacts from actual microstructural features was important for designing the  
182 final experimental method and ensuring more accurate measurements in following stages of the research.

183  
184 In order to explore this further, small areas of interest were chosen from the optical microscope examination and prepared for  
185 SEM imaging. Once each area is chosen, the whole slide was covered with foil, leaving a small hole approximately  $\sim 1\text{mm}^2$  in  
186 size in the foil which defines the area of interest (Figure 3). Since scanning might need to be repeated several times to get  
187 images with different resolutions and to prevent causing damage to the whole slide, only a small portion of a slide was prepared  
188 for imaging by coating with gold, and the scanning then carried out to image the selected feature.

189



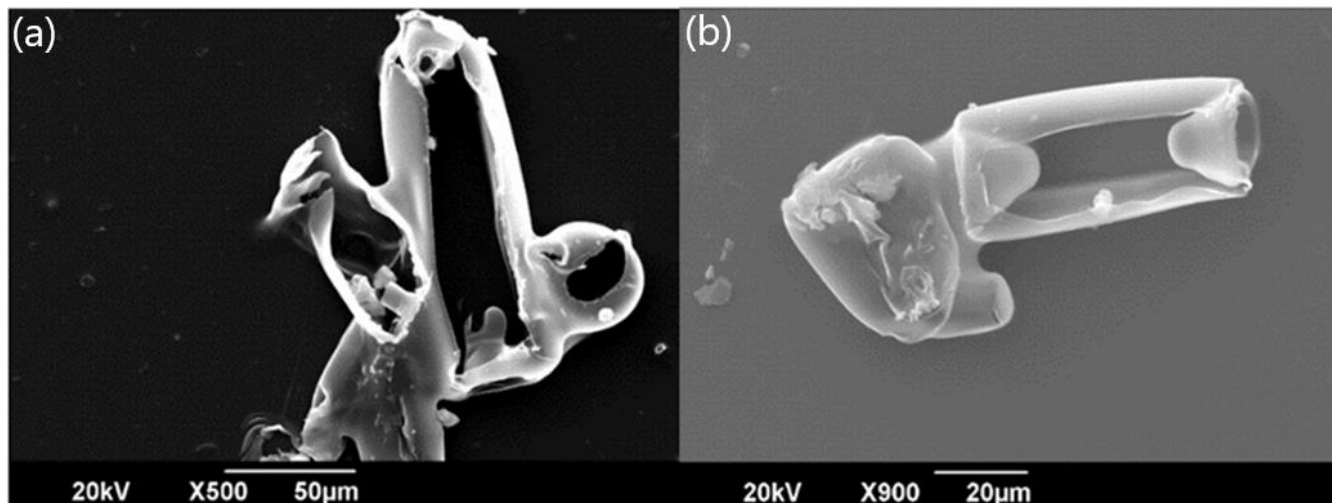
190

191 **Figure 3.** SEM imaging steps described: (a) sample 73 covered with foil with an opening on it, (b) the selected area's SEM image and (c)  
192 close-up image of 2 hexagonal plates that sit on each other.

193

194 In total, eight samples were prepared for this preliminary investigation, and were imaged with varying zoom scales during  
195 three different SEM sessions. When those images were examined thoroughly, it can be seen that a significant portion of the  
196 features are artefacts of the formvar process (Figure 4), that is the crystals did not form complete 3-dimensional replicas. One  
197 reason for this was considered to be the thin layer of formvar delivered by brushing it onto the slide, so there was insufficient  
198 depth for the crystals to be fully covered, or the shape and density of crystal could have prevented it sinking sufficiently for  
199 full cover. Finally, we had to consider whether the formvar material might start to deform after or whilst the ice crystals  
200 evaporated. A relatively simple workaround for much of these problems was to increase the depth of the formvar solution layer

201 by constructing a container to enable a pool of formvar to cover the slide, deep enough to capture the majority of single crystals,  
202 though it has consequences in terms of the evaporation rate as discussed previously.

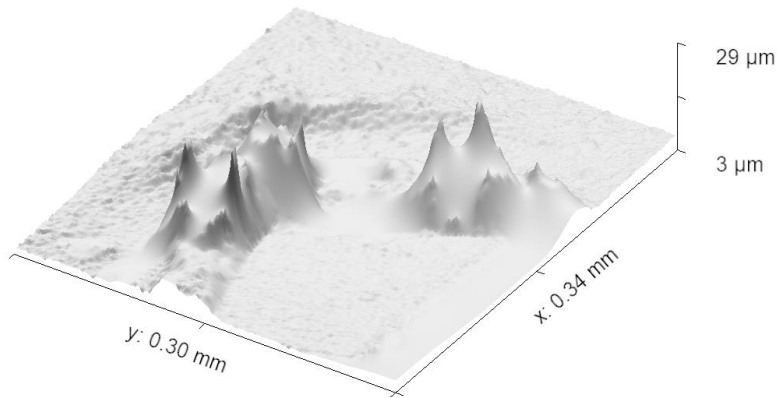


203  
204 **Figure 4.** SEM images of the ice crystals which did not sink fully into the formvar solution and consequently each replicas exhibits a hole  
205 in its upper surface.

### 206 3.1 Validation using salt crystals

207 Though the procedure described in Section 2 allowed us to measure the roughness of atmospheric ice crystals, an essential step  
208 is to ensure that the roughness values obtained from a replica are the same as would be measured from the crystal itself, that  
209 is to confirm that the formvar replica did not deform. To this end, the process was repeated with table salt (sodium chloride)  
210 crystals as a validation source, though with slight adaptations. **Initially, the brush technique was employed to create replicas  
211 to investigate surface structure. However, after analysis with optical profilometer, we found that the remaining surface details  
212 were incomplete or corrupted as shown in Figure 5 and did not provide any useful information about the surface characteristics,  
213 leading us to refine our approach. Therefore, we applied the formvar pool method discussed in methodology to produce further  
214 samples.**

215

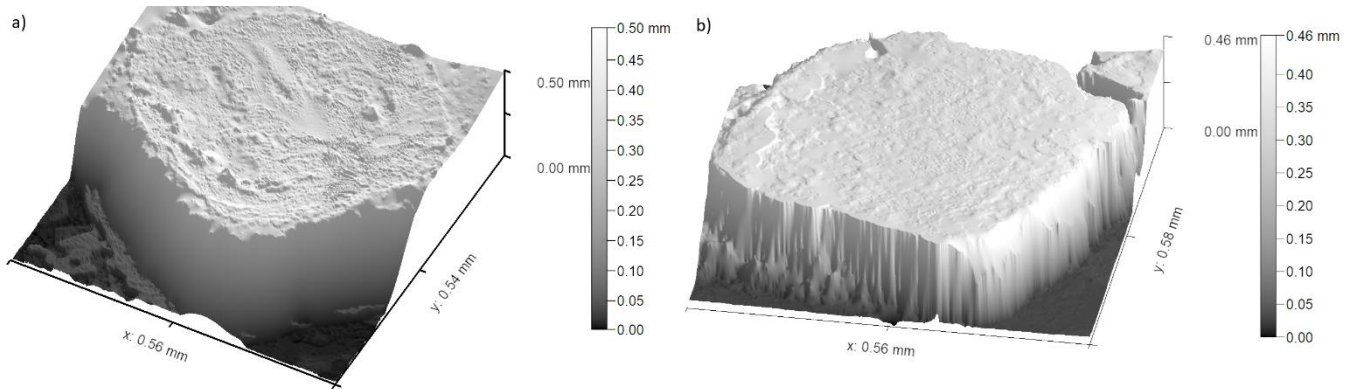


216

217 **Figure 5.** Surface scanning, using an optical profilometer, of a replica of salt crystal created by using brush technique. The image reveals  
 218 incomplete or distorted surface details due to limitations of the brush technique, which failed to capture fine structural features accurately.  
 219 This led to the refinement of the replication method

220

221 Once the chloroform had evaporated from the formvar solution, the formvar leaves behind a replica of the salt crystals. At this  
 222 stage though, the salt crystals remain and so must be removed by being dissolved in water. For this the sample slide was gently  
 223 placed in a water bath and left for 15 minutes until the salt dissolved and could be washed away. With the salt removed from  
 224 the sample, only the replica shell remained, and it was scanned with the SEM microscope. In addition, salt crystals from the  
 225 same batch were placed directly on a microscope slide and imaged and analysed in the same manner.



226

227 **Figure 6. (a)** Scan of a randomly chosen salt crystal without formvar solution application. **(b)** Scan of a randomly chosen formvar shell after  
 228 salt crystal removal. Both of them were taken with an optical profilometer.

229

230 The image in Figure 6 (left), shows the result scanning of a sample salt crystal without the application of formvar whereas the  
 231 right-hand side of the figure shows the result of the replica formvar process. In a comparison of both images, it can be seen  
 232 that a sufficient depth of formvar allows the full surface of the crystal to be imaged and complete scan of the surface retrieved.

233 This demonstrates our method's ability to capture the surface features effectively and provides a clear comparison of replicated  
234 surfaces despite the fact the sample salt crystals were not those subsequently covered in formvar and were randomly chosen.  
235 The results of the comparative roughness analysis of four salt crystals and four independent replicas are shown in Table 1.

236  
237 From these, we can see that the formvar replica process retains the roughness parameter measurement of the original crystal  
238 with a good level of accuracy. The deviation between the two samples is less than 5% which gives confidence that the  
239 measurement technique can represent true roughness parameters when it is applied to ice crystals. It should also be noted that  
240 salt crystals exhibit a range of roughness values, with the largest being approximately twice as large as the smallest in our  
241 samples, and this range is also seen in the replicas. This variability in roughness is also reflected in the replicas, despite the  
242 random selection of salt particles for measurement. These results provide confidence that the formvar replica technique can be  
243 applied effectively to characterize roughness parameters of ice crystals.

244 **Table 1.** 1D Roughness parameters of four salt crystals and four salt crystal replica samples.

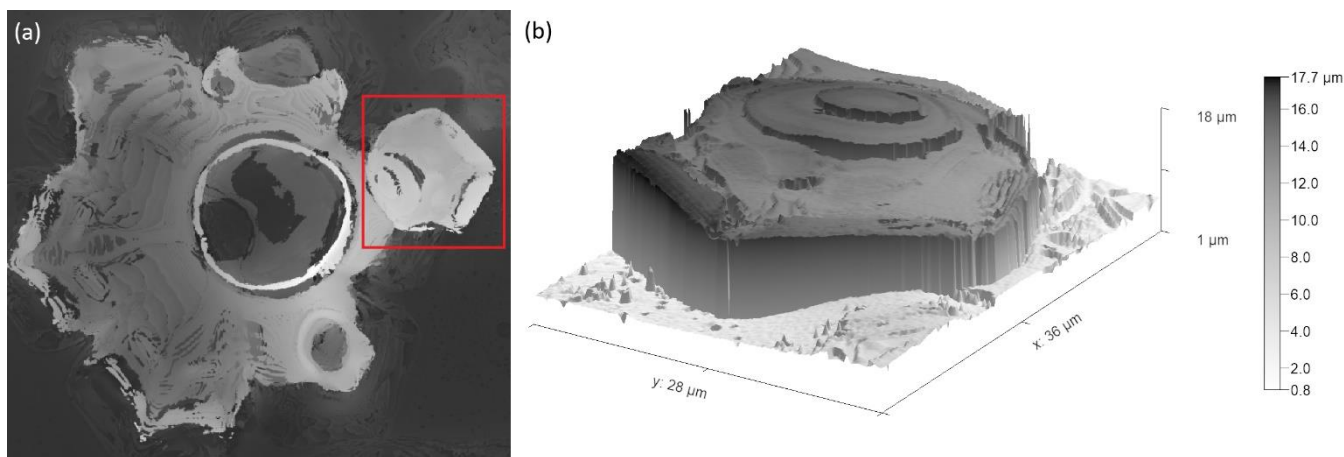
	Salt Crystal	Replica of Salt Crystal
Area	0.104 mm <sup>2</sup> to 0.255 mm <sup>2</sup>	0.1124 mm to 0.218 mm <sup>2</sup>
RMS Roughness	13.27 μm to 26.74μm	10.63 μm to 22.73μm
Mean Roughness	10.76 μm to 19.16 μm	8.27 μm to 18.96 μm
Skewness	-1.447 to -0.35	0.304 to 0.454

245  
246 The linear profiles used for roughness measurement were selected by making the scans for the full surface of each crystal, to  
247 make sure that all surface features were included. Although increasing the sample size would provide more robust statistical  
248 confidence, the use of four salt crystals provides a reasonable basis for comparison as they were covering full surface features.  
249 Skewness was measured using Gwyddion software, which calculated the surface asymmetry based on the height distribution  
250 of the features across the scanned profile, providing additional insight into the surface texture. A positive skewness indicates  
251 a surface dominated by peaks, while a negative skewness suggests deeper valleys. The observed skewness differences highlight  
252 variations in surface texture, which may influence properties such as adhesion, wettability, or mechanical interactions. Also,  
253 as a final check to make sure that these values are not significantly affected by the presence of formvar itself, a formvar surface  
254 with no crystals present was also scanned and analysed, the RMS roughness in this case being found to be 175 nm. This is  
255 orders of magnitude less than the values obtained in Table 1, supporting our assertion that the parameters retrieved from  
256 replicas are close to those for the original crystals.

### 257 3.2 Retrieval of Ice Crystal Roughness Parameters

258 At this stage, roughness parameters for ice crystals produced in the Manchester Ice Cloud Chamber (MICC) were explored  
259 following the procedures described in the methodology section. As a proof of concept for an experimental technique, rather

260 than a full treatise of ice crystal roughness, a single temperature ( $-20^{\circ}\text{C}$ ) was chosen for cloud formation and an ice cloud was  
 261 produced. In the cloud generation chamber, temperature and humidity are carefully controlled to initiate condensation under a  
 262 supersaturated environment, allowing water vapor to condense and form ice crystals and throughout this study, only one set of  
 263 environmental conditions is used. These crystals then fall and exit through an opening at the bottom of the chamber, where  
 264 they were captured, and replicas were created. The replicas were inspected with an optical profilometer rather than the SEM  
 265 described for early investigations due to improved speed, access and non-contact aspects of the method.  
 266



267  
 268 **Figure 7.** (a) One plate sits on another crystal marked with a red square. (b) Detail of surface scan of crystal highlighted by red square. Both  
 269 scans were taken with an optical profilometer.

270 An example crystal replica is shown in Figure 7, visually demonstrating that it is possible to capture the detailed surface  
 271 features and shape of ice crystals with formvar. Multiple ice crystals were analysed using the same software, Gwyddion, to  
 272 calculate roughness parameters and ascertain a range for the different variables. These results are shown in Table 2.

273 **Table 2.** Roughness parameters of three ice crystal replicas.  
 274

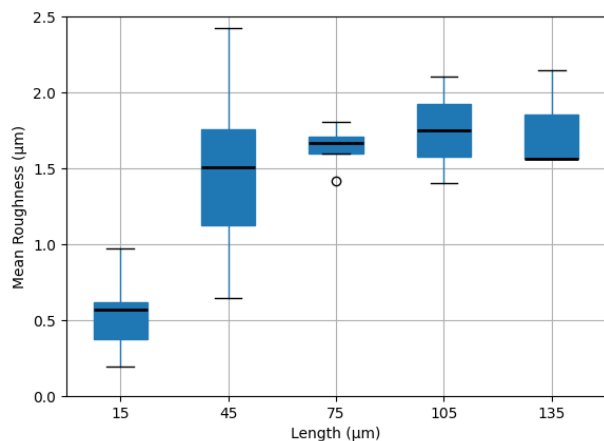
	Ice Crystal Replica
Area	$300\ \mu\text{m}^2$ to $800\ \mu\text{m}^2$
RMS Roughness	$1.2\ \mu\text{m}$ to $3.6\ \mu\text{m}$
Mean Roughness	$0.8\ \mu\text{m}$ to $2.66\ \mu\text{m}$
Skewness	-2.36 to 0.28

275  
 276 In using formvar to create ice crystal replicas, we were aware of the process of chemical etching which has been recognized  
 277 as a potential source of error in formvar replicas, as discussed in the previous studies (Sinha, 1977, 1978). This occurs when  
 278 water molecules which are weakly bonded can go into the formvar solution and leave artefacts called “etch-pits” that could

279 then be erroneously identified as crystal roughness . While we acknowledge these artefacts as a critical potential factor, we did  
280 not observe etching pits in our analysis.

281  
282 Roughness parameters were then compared over 35 randomly chosen areas from four different crystal surface scans to establish  
283 a correlation with the length parameter (side of the area scanned). By selecting various regions of the ice crystal surface,  
284 roughness can be analysed at different scales to provide a more detailed assessment of surface variability. In this study, multiple  
285 areas of different length parameter were chosen to capture localized variations, and their roughness values were statistically  
286 compared in order to consider different types of structural feature. The results, presented as a box plot in Figure 8, demonstrate  
287 the roughness distributions for each selected area, highlighting trends and potential correlations with the length parameter.

288



289  
290 **Figure 8.** Statistical comparison of length (µm) vs. mean-roughness values (µm) across multiple selected areas of multiple ice crystals'  
291 surfaces (n=7 for each size bin).

292  
293 In general, this distribution can be further simplified to show the correlation between length and roughness parameters. As the  
294 length increases, less frequent and larger features on the ice crystal surface are more likely to be captured and correspond to  
295 higher roughness values. The mean roughness plateaus at about 1.7 µm, indicating a limit to the small-scale roughness, with  
296 larger surface areas not capturing any greater roughness features.

297  
298 As before with the salt crystal analysis a range of roughness values are seen in the samples, though the range among means-  
299 roughness of size bins is not quite so large for our ice samples, only varying by a factor of 1.5–1.8 for over most of the size  
300 bins. However, we acknowledge that the environmental conditions are expected to have a significant effect on the roughness  
301 of ice crystals, particularly the supersaturation of the environment in which they form, and we have presented results from a  
302 single set of controlled conditions in developing this technique. Collier et al. (2016) used the roughness parameters of sand  
303 particles as a proxy for model work for asymmetry parameter calculations, yet it is encouraging that findings are relatively

304 close to the parameters in that work. Their two-scale roughness approach was applied to crystals with a size of 32.5  $\mu\text{m}$ , which  
305 lies between our lengths 15 and 45  $\mu\text{m}$ . The mean roughness for the large-scale features was measured at 1.08  $\mu\text{m}$ , while the  
306 mean roughness for the small-scale features was measured at 0.13  $\mu\text{m}$  which is approximately the lowest value that we  
307 observed with our smallest length scale of 15  $\mu\text{m}$ . In any event roughness will significantly affect the scattering behaviour of  
308 the crystals (Collier, et al., 2016), and this is often an underappreciated effect. In simple terms it can explain the relative rare  
309 of observance of halos in thin cirrus (Smedley, 2003; Forster and Mayer, 2022).

310

311 We stress that our study is a proof-of-concept study, and we anticipate that ice crystal roughness will vary with temperature,  
312 habit, and supersaturation. This variability is especially significant in high-altitude cirrus clouds and turbulent cumulus clouds,  
313 where the irregularities in ice crystals or droplets can lead to increased roughness, significantly impacting light scattering and  
314 the overall optical properties of the clouds. The high roughness can lead to higher scattering efficiencies and smaller asymmetry  
315 parameters (Ulanowski, et al., 2006), affecting the amount of solar radiation reflected back into space and complicating satellite  
316 retrievals of cloud properties. **The method presented here can be repeated under varying conditions which can provide an  
317 effective way to map the surface characteristics of ice crystals across different environmental conditions. By applying this  
318 technique to varying atmospheric settings, we can better understand how roughness evolves, which is essential for improving  
319 satellite observations, enhancing cloud property retrievals, and refining climate models that rely on precise knowledge of cloud  
320 dynamics.**

321

322 While this method was developed in a laboratory setting, it could potentially be adapted for airborne campaigns, once  
323 challenges of delivering the cloud particles to a protected formvar slide are overcome. The lower pressure available at altitude  
324 will assist rapid enough drying of the formvar, could be aided by slightly thinner coatings. Additionally, this method can be  
325 employed at some high-altitude ground-based stations situated at cloud level, allowing for the collection of samples directly  
326 from natural clouds. Such efforts are essential, as they can improve our understanding of cloud feedback mechanisms and the  
327 intricate details of roughness, ultimately contributing to a more comprehensive understanding of the net energy balance in the  
328 atmosphere.

329

330 **This method offers high-resolution and provides detailed structural information on ice crystal surface roughness despite the  
331 manual input required and the relatively limited ice crystal samples, compared with optical instruments like SID-3. While SID-  
332 3 is effective for airborne measurements, it gives an indirect measure of structure and roughness, while our offline approach  
333 allows for more precise analysis of surface roughness in a controlled environment. The two methods complement each other,  
334 with laboratory work providing detailed insight into ice crystal surface structure that can enhance future airborne studies.**

335

336 **Lastly, in terms of general roughness, providing similar results between actual crystal and its replica is important to ensure  
337 that this method can be used as a reliable proof-of-concept for future studies. While our current analysis simply uses one-**

338 dimensional roughness data, this study demonstrates the potential of this method to be improved and expanded to capture more  
339 comprehensive roughness characteristics. The consistency in roughness trends observed, despite the 1D measurement  
340 limitations, suggests that this method can be the basis for understanding ice crystal surface roughness. By building upon these  
341 results, we anticipate that future modifications in this technique will enable more precise evaluations by extracting complex  
342 roughness information to express crystal surface complexity under varying conditions.

#### 343 4 Conclusion

344 According to the IPCC report (2013), cloud models are inadequate for informing climate change models, which hinders the  
345 ability of models to provide accurate climate change predictions. Improvements are necessary in many aspects, especially with  
346 regard to their microphysical properties. The microphysical properties directly impact scattering characteristics. By  
347 representing the conditions of ice clouds accurately within models, reliability in predictions can be enhanced. While previous  
348 studies have extensively examined the shape and habits of ice particles, this study solely concentrates on a method for  
349 roughness parameter retrieval, leaving exploration of the effect of environmental conditions on roughness formation to future  
350 investigations.

351  
352 In calculating roughness parameters, this formvar technique, combined with modern imaging opportunities, offers novel  
353 possibilities for direct measurement of the roughness, despite its being based on an older technique. Roughness makes a critical  
354 contribution to scattering properties. Therefore, accurately determining roughness parameters can improve the prediction of  
355 scattering outcomes, which in turn can enhance cloud models and make their feedback to climate models more precise. Our  
356 method has resulted in the successful creation of ice crystal replicas, and their imaging and analysis at roughness scales by  
357 profilometer. The accuracy of the roughness parameters derived was validated through a comparative analysis using salt  
358 crystals, where the integrity of the crystals could be maintained independently of the formvar. This indicated that the roughness  
359 parameters found with our methodology have an uncertainty of no more than 5-6%, where some of this uncertainty may be  
360 natural variation in the salt crystals.

361  
362 A critical aspect of this study lies in its innovative integration of established techniques with cutting-edge instruments, which  
363 enables the extraction of valuable information on ice crystal roughness parameters. This research provides a detailed method  
364 for capturing and visualizing ice crystals captured in formvar using an optical profilometer, ensuring that key surface  
365 characteristics are preserved. Through comprehensive scanning, we have measured the roughness parameters. **Although the  
366 current work does not directly show the applicability of these one-dimensional roughness values to two-dimensional  
367 anisotropic rough surfaces or optical property calculations, it can be a foundation for future studies to provide such roughness  
368 parameters to be used in models and enhancing our understanding of cloud microphysics and their role in climate analysis.  
369 These findings can be also compared with both laboratory data and in-situ measurements, offering new perspectives on cloud  
370 microphysics. This work not only enhances our understanding of cloud behaviour but also contributes to refining models that  
371 simulate cloud properties, which are crucial for weather predictions and climate analysis. By bridging the gap between  
372 theoretical models and real-world observations, this study plays a key role in advancing our comprehension of cloud dynamics  
373 and their influence on the Earth's climate system.**

374  
375  
376

377 **Code Availability**

378 The Python code used to in this study is available from the corresponding author upon request.

379

380 **Data Availability**

381 The data used to support the findings of this study are available from the corresponding author upon request.

382

383 **Author Contribution**

384 Omer Celebi conceptualized and designed the study, conducted all data collection, analysis, and interpretation, and drafted the  
385 manuscript. Ann R. Webb, Paul Connolly and Andrew R.D. Smedley provided guidance, supervision, and critical revisions of  
386 the manuscript.

387

388 **Competing interests**

389 The contact author has declared that none of the authors has any competing interests.

390

391 **Acknowledgement**

392 This research was supported by a scholarship from the Ministry of National Education, Türkiye. I am grateful for their financial  
393 support, which made this work possible. The first author wrote the manuscript and improved the language with the help of  
394 generative AI. All other authors, who are native English speakers, reviewed and further improved the language of the  
395 manuscript.

396 **References**

- 397 (IPCC) I.: Climate change 2013: The physical science basis, Cambridge University Press, 2013.
- 398 (IPCC) I.: Climate change 2021: The physical science basis, Cambridge University Press, 923-1054, 2023.
- 399 Agar A. and Revell R.: A study of the formvar replica process, *British Journal of Applied Physics*, *British Journal of Applied*  
400 *Physics*, 1956.
- 401 Bailey M. and Hallett J.: A comprehensive habit diagram for atmospheric ice crystals: confirmation from the laboratory, *AIRS*  
402 *II*, and other field studies, *Journal of the Atmospheric Sciences*, 66, 9, 2888-2899, 2009.
- 403 Centre of Atmospheric Science, 2024.
- 404 Cheric .: Vapor pressure of chloroform, 1995.
- 405 Collier C., Hesse E., Taylor L., Ulanowski Z., Penttila A., Nousiainen T.: Effects of surface roughness with two scales on light  
406 scattering by hexagonal ice crystals large compared to the wavelength: DDA results, *Journal of Quantitative*  
407 *Spectroscopy & Radiative Transfer*, 182, 225-239, 2016.
- 408 Connolly P., Saunders C., Gallagher M., Bower K., Flynn M., Choulaton T., Whiteway J., Lawson R.: Aircraft observations  
409 of the influence of electric fields on the aggregation, *Quarterly Journal of the Royal Meteorological Society*, 131,  
410 608, 1695-1712, 2005.
- 411 Finnegan W. and Pitter R.: Atmospheric ice crystal processes, 1988.
- 412 Forster L. and Mayer B.: Ice crystal characterization in cirrus clouds III: retrieval of ice crystal shape and roughness from  
413 observations of halo displays, *Atmospheric Chemistry and Physics*, 22, 23, 15179–15205, 2022.
- 414 Gadelmawla E., Koura M., Maksoud T., Elewa I., Soliman H.: Roughness parameters, *Journal of Material Processing*  
415 *Technology*, 133-145, 2002.
- 416 Griggs D. and Jayaratne E.: The replication of ice crystals using formvar: techniques and precautions, *Journal of Atmospheric*  
417 *and Oceanic Technology*, 3, 3, 547-551, 1986.
- 418 Hong Y L.: The impact of two coupled cirrus microphysics–radiation parameterizations on the temperature and specific  
419 humidity biases in the tropical tropopause layer in a climate model, *Journal of Climate*, 2015.
- 420 Järvinen E., Wernli H., Schnaiter M.: Investigations of Mesoscopic Complexity of Small Ice Crystals in Midlatitude Cirrus,  
421 *Geophysical Research Letters*, 11, 465–11,472, 2018.
- 422 Kahler H., Lloyd B., Eden M.: Electron microscopic and other studies on a copper-cystine complex, National Cancer Institute,  
423 1951.
- 424 Kawamura P. and Mackay D.: The evaporation of volatile liquids, *Journal of Hazardous Materials*, 343-364, 1987.
- 425 Libbrecht K.: The physics of snow crystals, *Reports on Progress in Physics*, 68, 4, 855-895, 2005.
- 426 Magee N., Miller A., Amaral M., Cumiskey A.: Mesoscopic surface roughness of ice crystals pervasive across a wide range  
427 of ice crystal conditions, *Atmospheric Chemistry and Physics*, 12357–12371, 2014.

428 Magono C. and Chung W.: Meteorological classification of natural snow crystals, *Journal of the Faculty of Science, Hokkaido*  
429 *University. Series 7, Geophysics*, 321-335, 1966.

430 Miloshevich L. and Heymsfield A.: A balloon-borne continuous cloud particle replicator for measuring vertical profiles of  
431 cloud microphysical properties: instrument design, performance, and collection efficiency analysis, *Journal of*  
432 *Atmospheric and Oceanic Technology*, 14, 4, 753-768, 1997.

433 Revell R. and Agar A.: The preparation of uniform plastic films, *British Journal of Applied Physics*, 23, 1955.

434 Rucklidge J.: The examination by electron microscope of ice crystal nuclei from cloud chamber experiments, *Journal of the*  
435 *Atmospheric Sciences*, 301-308, 1965.

436 Saunders C. and Wahab N.: The influence of electric fields on the aggregation of ice crystals, *Journal of the Meteorological*  
437 *Society of Japan. Ser. II*, 53, 2, 121-126, 1975.

438 Schaefer V.: A method for making snowflake replicas, *Science*, 93, 2410, 239-240, 1941.

439 Sinha N.: Dislocations in ice as revealed by etching, *Philosophical Magazine*, 36, 6, 1385-1404, 1977.

440 Sinha N.: Observation of Basal Dislocations in Ice by Etching and Replicating, *Journal of Glaciology*, 21, 85, 385 - 395, 1978.

441 Smedley A.: Spectral scattering properties of cloud types, 2003.

442 Smith H., Connolly P., Baran A., Hesse E., Smedley A., Webb A.: Cloud chamber laboratory investigations into scattering  
443 properties of hollow ice particles, *Journal of Quantitative Spectroscopy and Radiative Transfer*, 157, 106-118, 2015a.

444 Smith H., Connolly P., Webb A., Baran A.: Exact and near backscattering measurements of the linear depolarisation ratio of  
445 various ice crystal habits generated in a laboratory cloud chamber, *Journal of Quantitative Spectroscopy and Radiative*  
446 *Transfer*, 178, 361-378, 2015b.

447 Ulanowski Z., Hesse E., Kaye P., Baran A.: Light scattering by complex ice-analogue crystals, *Journal of Quantitative*  
448 *Spectroscopy and Radiative Transfer*, 100, 1-3, 2006.

449 Ulanowski Z., Kaye P., Hirst E., Greenaway R., Cotton R., Hesse E., Collier C.: Incidence of rough and irregular atmospheric  
450 ice particles from Small Ice Detector 3 measurements, *Atmospheric Chemistry and Physics*, 1649–1662, 2014.

451 Voigtländer J., Chou C., Bieligk H., Clauss T., Hartmann S., Herenz P., Niedermeier D., Ritter G., Stratmann F., Ulanowski  
452 Z.: Surface roughness during depositional growth and sublimation of ice crystals, *Atmospheric Chemistry and*  
453 *Physics*, 13687–13702, 2018.

454 Warburton, J. A., Keyser, G., and Purcell, R. G.: A portable ice crystal replicator for use in snowfall transmission studies, *Opt.*  
455 *Eng. Cold Environ.*, 414, <https://doi.org/10.1117/12.935862>, 1983.